Journal of Membrane Science 320 (2008) 101–107

Contents lists available at ScienceDirect

Journal of Membrane Science

journal homepage: www.elsevier.com/locate/memsci

Bacterial attachment on reactive ceramic ultrafiltration membranes

Shannon Ciston[a], Richard M. Lueptow[b], Kimberly A. Gray[c,*]

[a] Department of Chemical and Biological Engineering, Northwestern University, 2145 Sheridan Road, Evanston, IL 60208, United States
[b] Department of Mechanical Engineering, Northwestern University, 2145 Sheridan Road, Evanston, IL 60208, United States
[c] Department of Civil and Environmental Engineering, Northwestern University, 2145 Sheridan Road, Evanston, IL 60208, United States

ARTICLE INFO

Article history:
Received 14 December 2007
Received in revised form 20 February 2008
Accepted 23 March 2008
Available online 6 April 2008

Keywords:
Biofilm
Titanium dioxide
Photocatalysis
Biofouling
Ultrafiltration

ABSTRACT

Bacterial attachment is an initial stage in biofilm formation that leads to flux decline in membrane water filtration. This study compares bacterial attachment among three photocatalytic ceramic ultrafiltration membranes for the prevention of biofilm formation. Zirconia ceramic ultrafiltration membranes were dip-coated with anatase and mixed phase titanium dioxide photocatalysts to prevent biofilm growth. The membrane surface was characterized in terms of roughness, hydrophobicity, bacterial cell adhesion, and attached cell viability, all of which are important factors in biofilm formation. The titanium dioxide coatings had minimal impact on the membrane roughness, reduced the hydrophobicity of membranes, prevented *Pseudomonas putida* attachment, and reduced *P. putida* viability. Degussa P25 is a particularly promising reactive coating because of its ease of preparation, diminished cell attachment and viability in solutions with low and high organic carbon concentrations, and reduced flux decline. These reactive membranes offer a promising strategy for fouling resistance in water filtration systems.

1. Introduction

Fouling is a major problem in membrane water filtration; it results in the loss of water throughput, increased energy usage, and system downtime for cleaning [1]. It is caused by the build-up of chemicals, bioorganic materials, and bacterial biofilms at the membrane surface [2]. The growing need globally to reuse low-quality waters with high organic and microbiological content requires separation technologies that resist fouling. The focus of this study was the fabrication and characterization of photoactive membrane surfaces coated with titanium dioxide for the prevention of bacterial attachment, an initial step in biofilm formation.

Bacteria preferentially live in microbial communities attached to surfaces, called biofilms, which are present throughout the environment. They become attached to a wide variety of materials and structures, including rocks, water intake pipes, medical implants, and filtration membranes. In many cases, these biofilms are a nuisance because of physical obstruction to flow (as in filtration) or enhanced corrosion of surfaces (as in pipes), and may present biological hazards (as in the attachment of a community of pathogens to a water distribution pipe) [3–5]. Being attached to surfaces may have several advantages over planktonic life for the bacterial communities, including access to greater nutrient levels, as chemicals tend to accumulate at surfaces, and protection from stressful conditions in solution, including biocidal agents and pH changes [6]. There are four steps in biofilm development: reversible bacterial attachment, irreversible attachment, cell reproduction and continued attachment, and production of the glycocalyx, the "slime" layer composed of exopolysaccharides and other chemicals found in the local bacterial environment [7]. Surface conditioning with organic chemical adsorption improves the rate of bacterial attachment, worsening the biofouling problem [8,9]. Hydrophobicity, roughness, and charge of the surface are factors that increase the likelihood of cell attachment and biofilm formation [10].

Titanium dioxide nanoparticles are well suited as a modification to membrane surfaces for the prevention of biofilm growth and fouling. First realized as a photocatalyst in the splitting of water, titanium dioxide is a semiconductor photocatalyst that converts radiant energy to chemical energy [11]. When titanium dioxide is irradiated by sufficiently energetic light, an electron is excited from the valence band to the conduction band, leaving behind a charge vacancy or hole. When these charges migrate to the nanoparticle surface, they can react with adsorbed species to produce highly reactive reducing and oxidizing radicals. In aqueous systems, the hole reacts with adsorbed hydroxyl groups to produce hydroxyl radicals which are non-specific, highly reactive oxidants [12].

Several crystal phases of titanium dioxide have been studied for photocatalysis; anatase and rutile crystal phase catalysts are used in this work. Anatase phase has been described as a more active phase because of slower rates of charge recombination, but it requires

* Corresponding author. Tel.: +1 847 467 4252; fax: +1 847 491 4011.
E-mail address: k-gray@northwestern.edu (K.A. Gray).

0376-7388/$ – see front matter © 2008 Elsevier B.V. All rights reserved.
doi:10.1016/j.memsci.2008.03.065

near-ultraviolet light of wavelength at most 385 nm for excitation. Rutile is the thermodynamically stable phase of titanium dioxide, and is excited by visible and ultraviolet light of wavelength less than 410 nm, but has a faster rate of charge recombination, making it less efficient as a photocatalyst compared to anatase [13,14]. The combination of these two phases in a mixed phase catalyst has been extensively studied, and produces a highly active catalyst [15,16]. Titanium dioxide has been experimentally tested in many environmental applications, including the degradation of organic chemicals in air and water systems, which take advantage of the highly reactive oxygen species generated in the presence of water [17,18]. More recently, a number of studies have shown that titanium dioxide drives the inactivation of bacteria, including *E. coli*, *E. cloacae*, *P. aeroginosa*, and *S. typhinusium* [19–25] in thin film and suspension applications.

Some contemporary research has coupled titanium dioxide reactivity with membrane filtration for water treatment. Ollis reviewed the literature reporting studies combining photocatalysis and membrane processes [26]. Most of these studies used titanium dioxide for organic treatment, and subsequently filtered the water with membranes. A few recent studies have explored the intimate coupling of titanium dioxide with the membrane materials, streamlining the water treatment process and taking advantage of the chemical and biological effects of titanium dioxide, considered here. For example, Choi et al. have applied a titanium dioxide catalyst toward the development of wastewater treatment systems appropriate for manned space missions [27]. They coated an alumina support (0.1 μm pores) with a sol–gel titanium dioxide coating and measured the photocatalytic activity of the coating and support with a variety of tests, including methylene blue degradation and *E. coli* inactivation in solution. They found that these modified membranes exhibited less flux decline over 60 min of exposure to organic-rich water. Madaeni and Ghaemi coated a thin-film composite membrane composed of polyvinyl alcohol, polyaryl sulfone ether, and polyester with a layer of Degussa P25 to create self-cleaning reverse osmosis membranes [28]. They found the coated membranes had higher whey flux after 4 h compared to virgin membranes.

This work is a detailed study of bacterial attachment and cell viability on photocatalytic membranes to identify membrane materials with potential for robust biofilm growth resistance. The effect of various titanium dioxide preparations on the surface properties of zirconia ultrafiltration membranes was evaluated, as measured by surface roughness and hydrophobicity. *Pseudomonas putida* bacterial attachment and cell viability on these membrane surfaces was tested with confocal laser scanning microscopy (CLSM) in solutions that mimic waters with both low and high organic carbon concentrations. Finally selected membranes were tested for flux decline after bacterial attachment.

2. Materials and methods

2.1. Preparation of composite membranes

Zirconia was chosen over alumina and titania as the ceramic membrane support because several reports have shown that close contact between zirconia and titania may boost the activity of titania photocatalysts [29,30]. Zirconia ceramic membrane discs were obtained from Sterlitech Corporation. These membranes discs have a layered structure, consisting of an alumina–titania–zirconia support material, and a zirconia pore size-controlling layer with a cut-off of 300 kDa (approximately 0.01 μm pore diameter), resulting in a water flow rate of 450–600 L/h m^2 at 1 bar trans-membrane pressure. The discs are 47 mm in diameter and 2.5 mm in thickness. They were rinsed with acetone and then rinsed thoroughly with deionized water to remove any surface impurities.

Zirconia discs were coated with one of three titanium dioxide catalysts. The catalysts included Degussa P25 (80% anatase, 20% rutile), anatase phase sol–gel, and mixed phase sol–gel (91% anatase, 9% rutile). Degussa P25 is a highly characterized commercial catalyst produced by high-temperature flame hydrolysis, with heterogeneous phase composition (15–30% rutile, remainder anatase) and particle size (primary particle size 30 nm, aggregates up to 200 nm). It is considered by many to be the "gold standard" of photocatalysts because of its high reactivity [31]. Sol–gel catalysts were prepared by solvothermal processing using a titanium tetraisopropoxide precursor in ethanol sol, as described previously [32]. These sol–gel catalysts have a primary particle size of 20–30 nm diameter and have demonstrated higher levels of photoreactivity compared to Degussa P25 when tested in slurry systems for methylene blue degradation [33]. All catalysts were applied to discs by dip-coating in a slurry of 0.1 g/L catalyst, and 0.05 g/L dioctyl sulfosuccinate surfactant in water [34]. After sonicating the slurry for 1 h, the top surface of each disc was dipped into the slurry and withdrawn by hand at a rate of about 3 cm/s. Discs were dried in a 105 °C oven for 2.5 h, and then heat treated in a furnace with a ramp rate of 5 °C/min to 450 °C, held there for 1 h, and then cooled slowly to room temperature. This process was repeated until 4 mg of the catalyst had been deposited on the disc surface (about 5 repetitions). Catalyst phase composition was confirmed after deposition and heat treatment by grazing incidence X-ray e ATX-G diffractometer outfitted with a high intensity 18 kW copper X-ray source.

2.2. Membrane roughness

The roughness of each disc was analyzed using JEOL Scanning Probe Microscope JSPM-5200 in AC tapping mode. Atomic force microscope (AFM) images from 5 different regions on each sample surface were collected. The scanning area was increased until roughness measurements were constant at 15 μm × 15 μm sections using a scan speed of 1 ms, filter of 1.4 Hz, and loop gain of 4, with a silicon nitride probe tip. Root mean square (RMS) roughness was determined for each sample using the JEOL WinSPM Processing Software.

2.3. Membrane hydrophobicity

The hydrophobicity of the titania coatings was compared to evaluate how the coatings affected the molecule adsorption at the membrane surface. Hydrophobicity was measured using sessile water drop shape analysis on the titania coatings. Because the porous membranes made measurement difficult, nonporous glass slides were used as supports for the catalyst particles. Deionized water was dropped onto the surface of the glass slide at a rate of 3 μL/min, to form droplets of ~0.5 μL, with Krüss model DSA100 drop shape analysis system. The sessile water drop contact angle was determined using a circle-fitting method. Five measurements were taken on each sample, including glass slides coated first with zirconia and then with the catalyst, and a set of controls including uncoated glass slides, glass slides with catalysts applied, and glass slides with zirconia coating.

2.4. Cell attachment and viability

P. putida is a Gram-negative, rod-shaped bacterium. It was chosen as the bacterial model because *P. putida* is commonly present throughout the environment and readily colonizes biofilms [35,36]. The American Type Culture Collection *P. putida* type strain number 12633 was incubated in a solution of 10% R2A media [37] and

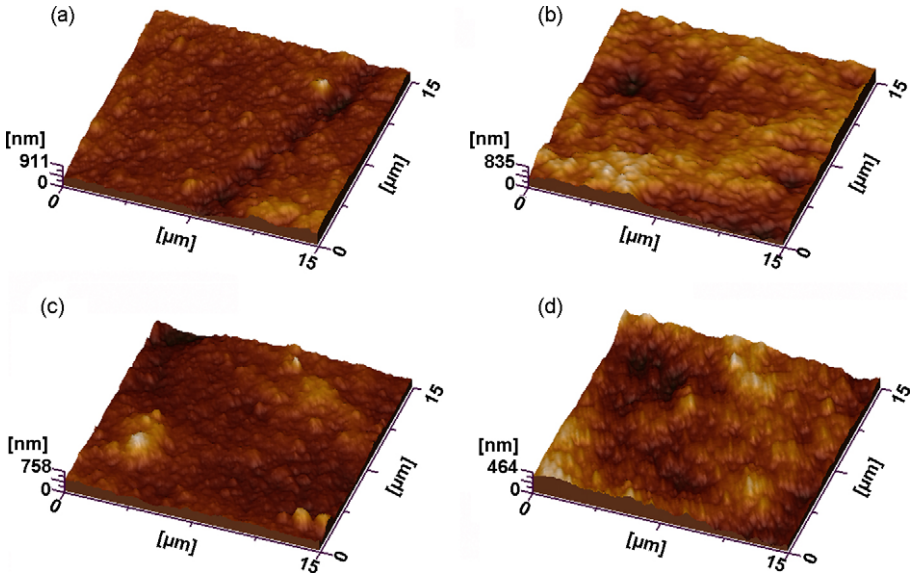

Fig. 1. AFM images of (a) uncoated zirconia disc; (b) Degussa P25-coated disc; (c) sol–gel anatase-coated disc; (d) sol–gel mixed phase-coated disc.

90% phosphate buffer solution (PBS) at 28 °C, rotating at 100 rpm until it reached the exponential growth phase, at a concentration of about 10^8 colony forming units per milliliter (CFU/mL). This solution was diluted in sterile PBS to bring the solution cell concentration to approximately 10^6 CFU/mL, and the total organic carbon (TOC) concentration level to approximately 1 mg/L. These carbon and bacterial cell concentrations are typical of oligotrophic, fresh surface waters [38,39]. TOC was measured using an Apollo 9000 TOC Combustion Analyzer.

Disc samples 0.5–1 cm^2 in size were taken from each type of coated membrane plus an uncoated control. These samples were sterilized in 20 mL beakers, and 10 mL of the dilute cell culture was added. These samples were rotated at 100 rpm on an orbital shaker, while being illuminated with a UVP Blak-Ray Lamp, model B 100 AP, with peak intensity at 365 nm. Samples were illuminated for 3 h at 10 cm below the lamp and 6 cm radially outward from the center spot, with a light intensity of 10 µmol/m^2 s (~330 µW/cm^2), as measured by Apogee Quantum Meter model QMSW-SS. Control samples were prepared identically and kept in dark conditions for 3 h.

After illumination, the disc samples were removed from solution and stained using Invitrogen Molecular Probes Live/Dead stain containing Styo-9 nucleic acid and propidium iodide to mark attached cells as either having intact (live) or ruptured (dead) cell membranes. Samples were maintained in PBS at 4 °C for microscopy. The concentration of the cell culture in the beaker above each disc was also measured using standard plate counting technique.

The amount and viability of attached cells were imaged using confocal laser scanning microscopy. An upright Leica confocal microscope, model DM RXE-7, outfitted with a 40× dipping lens was used with Ar 488 nm and GreNe 543 nm lasers to excite the live/dead stain. A stack of digital images was collected at 1-µm intervals through the vertical direction of the sample in two channels (live and dead) cells throughout the biomass at the surface of the disc. Image J software was used to analyze the images through the use of the threshold function to quantify the amount of live (stained green) and dead (stained red) cell attachment present in each sample. Each sample was analyzed in five (375 µm × 375 µm) sections. A second trial of this entire process validated the results with a high degree of reproducibility.

Throughout the results and discussion section of this paper, the heteroscedastic *t*-test was applied to determine differences between average sample values at a confidence interval of 90% [40]. The heteroscedastic *t*-test is appropriate for use in cases when

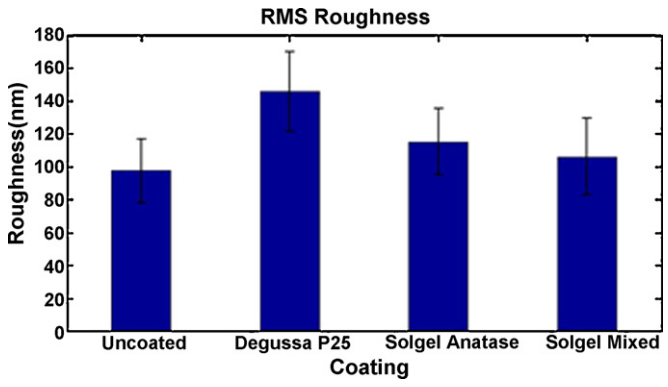

Fig. 2. RMS roughness as measured by AFM over 5 sample regions showing Degussa P25 coatings were slightly rougher than uncoated discs, but sol–gel coatings did not change the surface roughness.

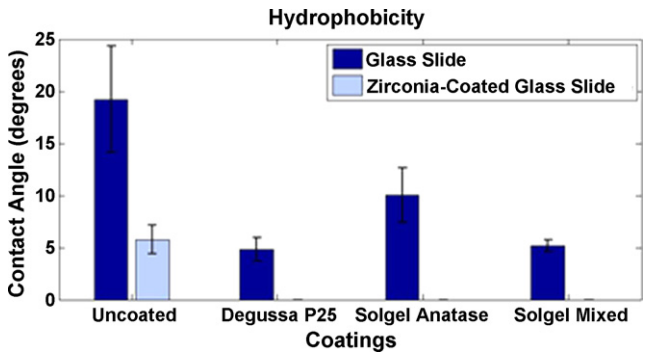

Fig. 3. Comparison of contact angle, showing the decrease in hydrophobicity for titania-coated slides. Note that contact angles on slides coated first with zirconia and then titania were below measurement limits, indicating a completely hydrophilic surface.

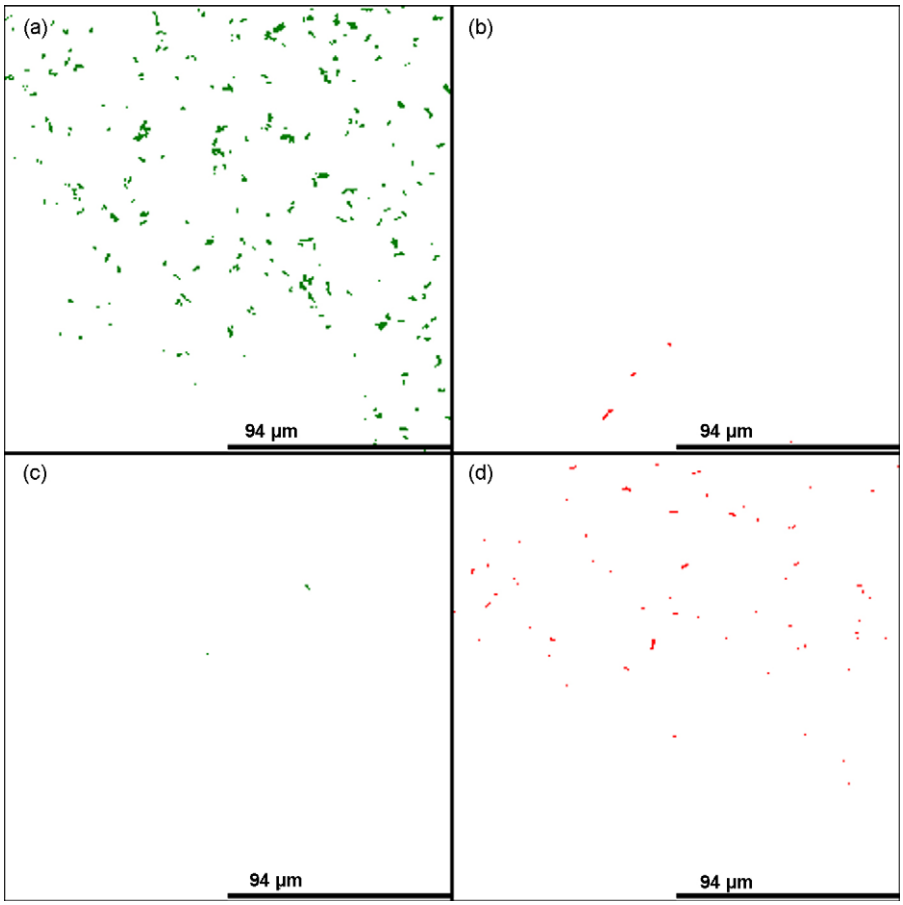

Fig. 4. Typical images from confocal microscope divided into live and dead channel signals. Live cells are displayed in green, while dead cells are displayed in red. (a) Control sample (uncoated, dark) live cell image; (b) control sample (uncoated, dark) dead cell image; (c) illuminated Degussa P25 sample live cell image; (d) illuminated Degussa P25 sample dead cell image. (For interpretation of the references to color in this figure legend, the reader is referred to the web version of the article.)

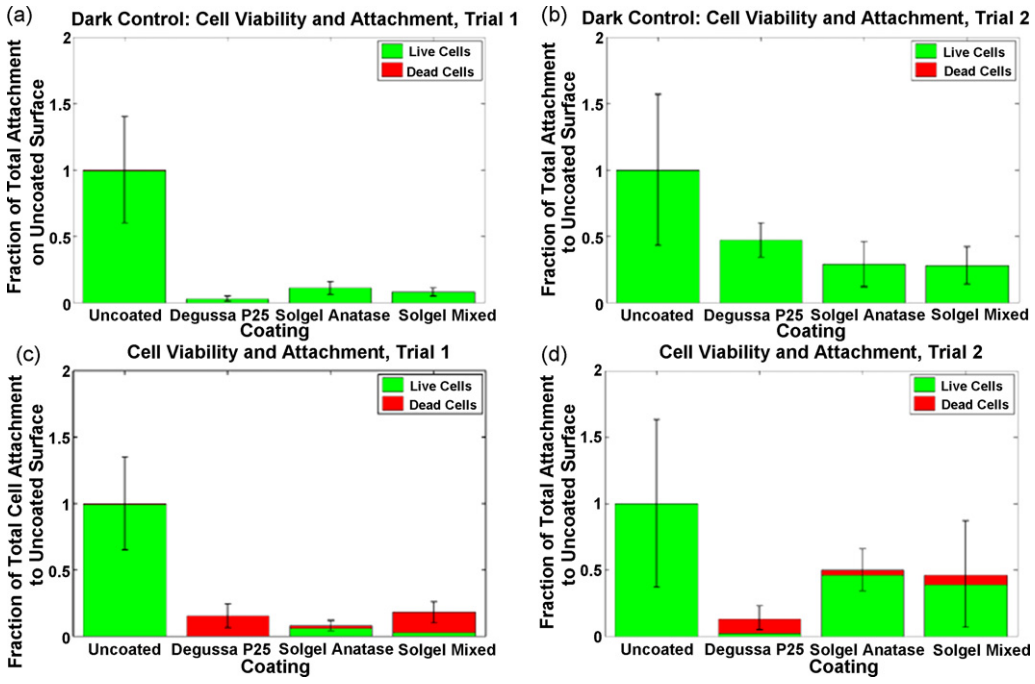

Fig. 5. All images show attachment normalized to the total attachment on an uncoated disc for the respective trial (a) dark control trial #1; (b) dark control trial #2; (c) illuminated trial #1; (d) illuminated trial #2.

sample populations are less than 30 and when unknown variances of two populations are not equal.

3. Results and discussion

3.1. Membrane roughness

Atomic force microscopy images are shown in Fig. 1. Roughness measurements by AFM indicate that some catalyst coatings may yield a small increase in surface roughness, as shown in Fig. 2.

The roughness of the P25 coating was somewhat greater than that of the uncoated membrane, with an average roughness of 146 nm compared to 98 nm. However, there was no significant difference between the uncoated surface and the sol–gel-coated surfaces, with the average anatase roughness of 115 nm and the average mixed phase roughness of 106 nm.

A number of studies spanning the medical, filtration, and coating fields have shown the effect of surface roughness on bacterial adhesion or attachment. Litzler et al. found that *S. epidermis* and *P. aeruginosa* adhesion to heart valves was dependent on the surface roughness within the range of 9–35 nm [41]. Ghayeni et al. reported increased wastewater bacterial attachment with increased RO membrane roughness [42]. Li and Logan tested the adhesion of eight different bacterial strains, including *E. coli* and *P. aeruginosa*, to 11 different glass and metal oxide surfaces (roughness 4.1–17.6 nm). They found no significant effect of surface roughness on bacterial attachment, but identified potential trends in the data that may suggest a correlation: the roughest surfaces bore maximum attachment, and there was little variation among the bacterial strains in attachment to the smoothest surfaces. They concluded that there may be ranges of roughness over which bacterial adhesion is correlated with roughness, and other ranges over which adhesion is not correlated with roughness [3]. The attachment results for this study are detailed in Section 3.3.

3.2. Membrane hydrophobicity

The average water drop contact angle measured for clean glass slides was 19°. A wide range of hydrophilic water drop contact angles have been reported for glass; this measurement falls within the reported range, and serves as a point of comparison for the coated glass slides in this study [3,43,44]. The glass contact angle was much greater than the average contact angles on glass slides coated with Degussa P25 (5°), sol–gel anatase (10°), and sol–gel mixed phase (5°), as shown in Fig. 3 (dark blue).

Titanium dioxide coatings resulted in a highly hydrophilic surface. When glass slides were coated first with zirconia (the surface of the membrane discs), there was a similar reduction in hydrophobicity, with a contact angle of 6° (light blue). Further coating of this surface with titania catalysts, however, yielded a completely hydrophilic surface with contact angles below measurement limits, suggesting that the attachment of organic molecules on the titania-coated membrane surface will be less favorable than attachment on the uncoated membrane surface.

Previous studies of titania photocatalysts have shown superhydrophilic characteristics of titanium dioxide films under UV illumination; similar results may be found when our coatings are illuminated [45]. The reduced hydrophobicity of the titania-coated membranes may play a key role in hindering bacterial attachment.

3.3. Bacterial cell attachment and viability

Fig. 4 shows typical confocal microscope images from the control sample (uncoated in the dark, a and b) and from an experimental sample (illuminated sample coated with Degussa P25, c and d), after being processed through a threshold filter to remove background noise. The color assigned to the live and dead cells follows from the color at which the stained cells fluoresce under laser excitation: live cells are shown in green while dead cells are shown in red. The completely untreated sample showed a high degree of bacterial attachment with strong cell viability (Fig. 4a and b). In contrast, the disc coated with Degussa P25 showed very sparse cell attachment and a high degree of cell inactivation (Fig. 4c and d), which would prevent new cell or biofilm growth.

In both the dark control tests and in the illuminated experimental tests, there was significantly less *P. putida* attachment to samples coated with all types of titania catalyst compared to the plain zirconia disc. In Fig. 5, average results are represented as a fraction of the total attachment on the uncoated control sample in each test. Because a new bacterial colony was used for each trial, it is most appropriate to compare results within an experiment using the same colony. The attachment was measured as the total volume of live or dead cell pixels summed through all vertical image slices near the membrane surface.

Based on the data in Fig. 5a, the coated discs each had less than 12% of the total attachment of the uncoated disc. In the second trial shown in Fig. 5b, each of the coated discs had less than 47% of the total attachment of the uncoated disc, repeating the trend of the first trial, though to a lesser degree. The reduction in dark attachment can be attributed to the diminished hydrophobicity of the titania-coated surface. Furthermore, the increase in surface roughness imparted by the Degussa P25 did not appear to be an important factor in cell attachment in this system. The cell viability for all samples in the dark tests was at least 94%, leaving the membranes vulnerable to cell reproduction at the surface.

In Fig. 5c coated samples had less than 20% of the uncoated attachment. In Fig. 5d coated samples had less than 50% of the attachment on the uncoated sample. Irradiation yielded dramatic effects on the cell viability on the reactive surfaces, as shown in Fig. 5c and d. In the first trial (Fig. 5c) there was only 2% viability on Degussa P25, 70% viability on sol–gel anatase, and 18% viability on sol–gel mixed phase surfaces, in comparison to 98% cell viability of the uncoated control sample. Similarly, in the second trial (Fig. 5d) there was 99% viability on the uncoated sample, a mere 20% viability on Degussa P25, 94% viability on sol–gel anatase, and 86% viability on sol–gel mixed surfaces. Image analysis required a great deal of time for these experiments, so additional trials were not completed after achieving consistent results in two trials.

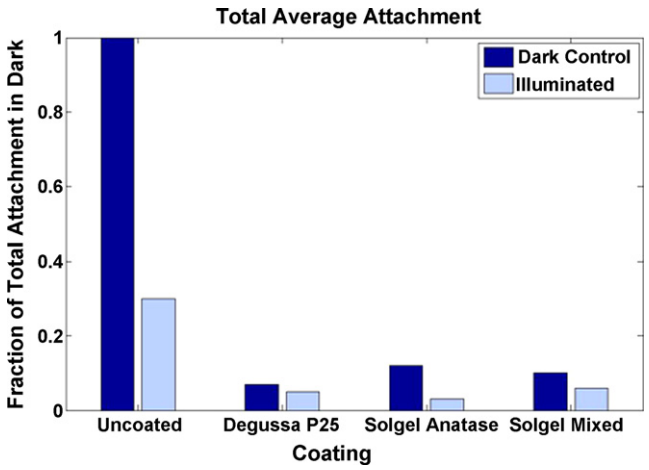

Fig. 6. Average of dark controls attachment compared to average of illuminated attachment, results shown as fraction of total average attachment in the dark.

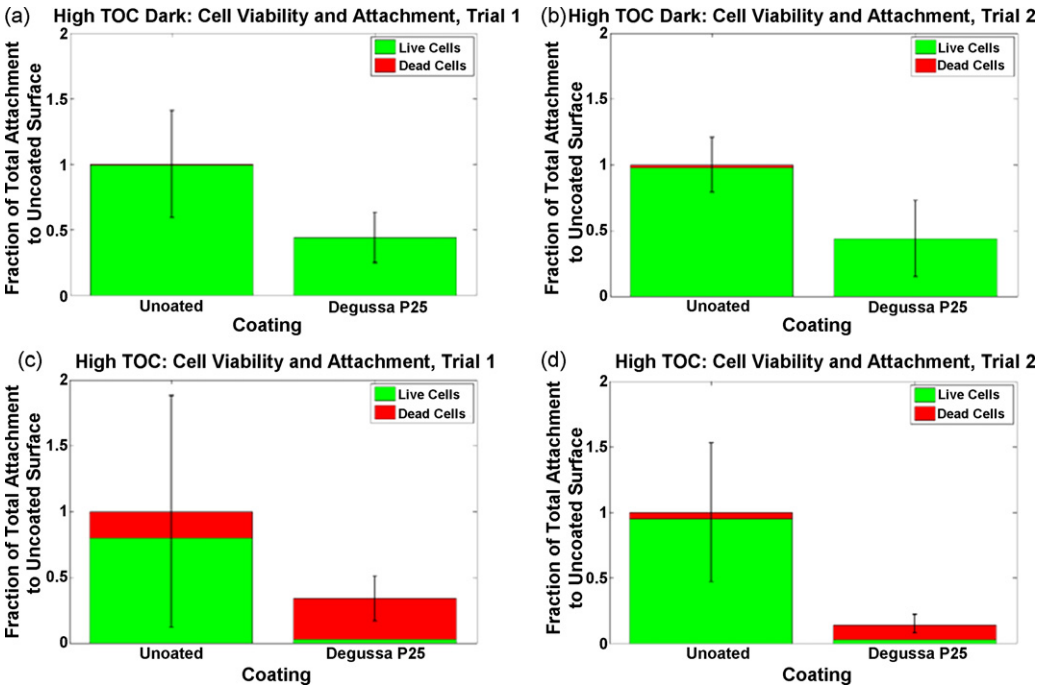

Fig. 7. All images show attachment normalized to the total attachment on an uncoated disc for the respective trial (a) high TOC dark control trial #1; (b) high TOC dark control trial #2; (c) high TOC illuminated trial #1; (d) high TOC illuminated trial #2.

Under these experimental conditions, the light intensity was sublethal to the *P. putida*; plate counts showed that the concentration of cells in solution remained constant at approximately 10^6 CFU/mL throughout the experiments, indicating that the higher ratio of dead cells at the reactive membrane surfaces was a surface effect. Preliminary results, however, indicated that doubling the light intensity resulted in 1-log kill of *P. putida* in the solution for Degussa P25 samples.

Like all living organisms, *P. putida* is complex, such that each culture is unique, even when incubated under identical conditions and harvested at the same growth stage. For this reason, one cannot rigorously compare the degree of attachment in trials in the dark (with a given batch of cells) to attachment in trials under illumination (with a different batch of cells) in the present experimental design. Nevertheless, comparing the average cell attachment under dark conditions to that under illuminated conditions, shown in Fig. 6, the data suggest that illumination alone may result in some reduction of attached cells. While the ultraviolet light alone had an inhibitory effect on cell division in the illuminated samples, the light effect was amplified by the photocatalyst.

When metal oxide materials are coated with organic chemicals or surfactants, the hydrophobicity of the surface increases [46,47]. Increased hydrophobicity has been linked to higher levels of bacterial attachment and to membrane fouling [1,3]. Higher levels of organic carbon content in natural source waters contribute to membrane fouling, possibly because these organics modify the hydrophobicity of the membrane surface [2]. Humic substances including humic and fulvic acids are commonly occurring classes of natural organic carbon, having an amphiphilic structure with hydrophobic and hydrophilic moieties [48]. Jucker and Clark found that humic substances altered the hydrophobicity of a hydrophobic membrane due to their orientation at the membrane surface [49]. Similarly, humic substances would increase the hydrophobicity of the membrane surface here if the hydrophilic moieties of the acid were to orient themselves at the hydrophilic surface, leaving the hydrophobic backbone exposed to the solution. The photocatalyst coating oxidizes the organic materials at the membrane surface, thereby retarding both their adsorption and positive effect on bacterial attachment.

To examine the effects of an organic-rich water on the reactive membranes, the cell attachment and viability experiment was repeated for uncoated and Degussa P25-coated samples in a high TOC solution, where PBS solution was amended with 34 mg/L Suwannee River fulvic acid to bring the solution to 24 mg/L TOC.The results, shown in Fig. 7, illustrate that Degussa P25 maintained its effectiveness and produced a dramatic reduction in cell attachment and viability even at elevated organic concentrations.

An important result of reduction in cell attachment and subsequent biofilm growth is the prevention of flux decline across the membrane during filtration. Preliminary results show that after the 3-h illuminated attachment test, the Degussa P25 discs displayed 10% less flux decline than uncoated membrane discs (average of three trials). This effect will be studied further in future experimental work.

4. Conclusion

This work demonstrates the use of photocatalysts to reduce cell attachment and viability on ceramic ultrafiltration membranes. Degussa P25 coatings reduced the hydrophobicity of the surface, and prevented cell attachment in low and high TOC environments. Further, these coatings inactivated cells at the membrane surface and may prevent flux decline. Degussa P25 is commercially available, and can be applied to membranes using a simple dip coating process; for this application, nanoparticles of titanium dioxide synthesized by the sol–gel techniques did not show enhanced reactivity over P25. Ultraviolet light alone had an inhibitory effect on cell division, while titania coatings alone (no illumination) reduced cell attachment due to reduction in hydrophobicity. The combination of these factors produced a reactive system with greatly diminished cell attachment and strong levels of cell inactivation, to create a membrane surface with great promise for the

prevention of biofilm growth. These membranes have potential to provide a robust solution to the persistent problem of membrane fouling.

Acknowledgements

This study was based upon work supported by the National Science Foundation under Grant No. 0403581. Thanks to Evonik Degussa for their generous donation of P25. The XRD work was performed in the J.B. Cohen X-ray Diffraction Facility at Northwestern University. The AFM work was performed in the NIFTI facility of NUANCE Center at Northwestern University. NUANCE Center is supported by NSF-NSEC, NSF-MRSEC, Keck Foundation, the State of Illinois, and Northwestern University. The confocal microscopy work was performed in the Biological Imaging Facility on the Evanston campus of Northwestern University. Thanks to Martina Hausner, William Russin, Jerry Carsello, Gonghu Li, Yuan Yao, Jessica Kunke, Andrew Reiter, and Virginia Palmer for assistance with experimental work.

References

[1] M.F.A. Goosen, S.S. Sablani, H. Ai-Hinai, S. Ai-Obeidani, R. Al-Belushi, D. Jackson, Fouling of reverse osmosis and ultrafiltration membranes: a critical review, Separation Science and Technology 39 (2004) 2261–2297.
[2] B. Van der Bruggen, C. Vandecasteele, T. Van Gestel, W. Doyen, R. Leysen, A review of pressure-driven membrane processes in wastewater treatment and drinking water production, Environmental Progress 22 (2003) 46–56.
[3] B.K. Li, B.E. Logan, Bacterial adhesion to glass and metal-oxide surfaces, Colloids and Surfaces B-Biointerfaces 36 (2004) 81–90.
[4] S.J. Yuan, S.O. Pehkonen, Microbiologically influenced corrosion of 304 stainless steel by aerobic *Pseudomonas* NCIMB 2021 bacteria: AFM and XPS study, Colloids and Surfaces B-Biointerfaces 59 (2007) 87–99.
[5] S.L. Percival, J.T. Walker, Potable water and biofilms: a review of the public health implications, Biofouling 14 (1999) 99–115.
[6] Y.A. Nikolaev, V.K. Plakunov, Biofilm—"city of microbes" or an analogue of multicellular organisms? Microbiology 76 (2007) 125–138.
[7] W.M. Dunne, Bacterial adhesion: seen any good biofilms lately? Clinical Microbiology Reviews 15 (2002) 155–166.
[8] T. Boland, R.A. Latour, F.J. Sutzenberger, Molecular basis of bacterial adhesion, in: Y.H. An, R.J. Friedman (Eds.), Handbook of Bacterial Adhesion: Principles, Methods and Applications, Humana Press, Totowa, NJ, 2000.
[9] R. Bos, H.C. van der Mei, H.J. Busscher, Physico-chemistry of initial microbial adhesive interactions—its mechanisms and methods for study, FEMS Microbiology Reviews 23 (1999) 179–230.
[10] S. Kang, E.M.V. Hoek, H. Choi, H. Shin, Effect of membrane surface properties during the fast evaluation of cell attachment, Separation Science and Technology 41 (2006) 1475–1487.
[11] A. Fujishima, K. Honda, Electrochemical photolysis of water at a semiconductor electrode, Nature 238 (1972) 37–38.
[12] D.M. Blake, J. Webb, C. Turchi, K. Magrini, Kinetic, Mechanistic overview of TiO_2-photocatalyzed oxidation reactions in aqueous-solution, Solar Energy Materials 24 (1991) 584–593.
[13] A. Mills, S. LeHunte, An overview of semiconductor photocatalysis, Journal of Photochemistry and Photobiology A-Chemistry 108 (1997) 1–35.
[14] M.A. Fox, M.T. Dulay, Heterogeneous photocatalysis, Chemical Reviews 93 (1993) 341–357.
[15] D.C. Hurum, A.G. Agrios, K.A. Gray, T. Rajh, M.C. Thurnauer, Explaining the enhanced photocatalytic activity of Degussa P25 mixed-phase TiO_2 using EPR, Journal of Physical Chemistry B 107 (2003) 4545–4549.
[16] G. Li, K.A. Gray, The solid–solid interface: explaining the high and unique photocatalytic reactivity of TiO_2-based nanocomposite materials, Chemical Physics 339 (2007) 173–187.
[17] M.R. Hoffmann, S.T. Martin, W.Y. Choi, D.W. Bahnemann, Environmental applications of semiconductor photocatalysis, Chemical Reviews 95 (1995) 69–96.
[18] K. Pirkanniemi, M. Sillanpaa, Heterogeneous water phase catalysis as an environmental application: a review, Chemosphere 48 (2002) 1047–1060.
[19] G. Gogniat, M. Thyssen, M. Denis, C. Pulgarin, S. Dukan, The bactericidal effect of TiO_2 photocatalysis involves adsorption onto catalyst and the loss of membrane integrity, FEMS Microbiology Letters 258 (2006) 18–24.
[20] B. Kim, D. Kim, D. Cho, S. Cho, Bactericidal effect of TiO_2 photocatalyst on selected food-borne pathogenic bacteria, Chemosphere 52 (2003) 277–281.
[21] K. Sunada, T. Watanabe, K. Hashimoto, Studies on photokilling of bacteria on TiO_2 thin film, Journal of Photochemistry and Photobiology A-Chemistry 156 (2003) 227–233.
[22] K. Onoda, J. Watanabe, Y. Nakagawa, I. Izumi, Photocatalytic bactericidal effect of powdered TiO_2 on *Streptococcus-mutans*, Denki Kagaku 56 (1988) 1108–1109.
[23] Y. Kikuchi, K. Sunada, T. Iyoda, K. Hashimoto, A. Fujishima, Photocatalytic bactericidal effect of TiO_2 thin films: dynamic view of the active oxygen species responsible for the effect, Journal of Photochemistry and Photobiology A-Chemistry 106 (1997) 51–56.
[24] B. Kepenek, U.O.S. Seker, A.F. Cakir, M. Urgen, C. Tamerler, Photocatalytic bactericidal effect of TiO_2 thin films produced by cathodic arc deposition method, Bioceramics 16 (2004).
[25] J.A. Ibanez, M.I. Litter, R.A. Pizarro, Photocatalytic bactericidal effect of TiO_2 on *Enterobacter cloacae*. Comparative study with other Gram (−) bacteria, Journal of Photochemistry and Photobiology A-Chemistry 157 (2003) 81–85.
[26] D.F. Ollis, Integrating Photocatalysis and Membrane Technologies for Water Treatment, Advanced Membrane Technology, 2003.
[27] H. Choi, E. Stathatos, D.D. Dionysiou, Photocatalytic TiO_2 films and membranes for the development of efficient wastewater treatment and reuse systems, Desalination 202 (2007) 199–206.
[28] S.S. Madaeni, N. Ghaemi, Characterization of self-cleaning RO membranes coated with TiO_2 particles under UV irradiation, Journal of Membrane Science 303 (2007) 221–233.
[29] J.H. Schattka, D.G. Shchukin, J.G. Jia, M. Antonietti, R.A. Caruso, Photocatalytic activities of porous titania and titania/zirconia structures formed by using a polymer gel templating, Chemistry of Materials 14 (2002) 5103–5108.
[30] Y.M. Wang, S.W. Liu, M.K. Lu, S.F. Wang, F. Gu, X.Z. Gai, X.P. Cui, J. Pan, Preparation and photocatalytic properties of Zr^{4+}-doped TiO_2 nanocrystals, Journal of Molecular Catalysis A-Chemical 215 (2004) 137–142.
[31] D.C. Hurum, K.A. Gray, T. Rajh, M.C. Thurnauer, Recombination pathways in the Degussa P25 formulation of TiO_2: surface versus lattice mechanisms, Journal of Physical Chemistry B 109 (2005) 977–980.
[32] G. Li, K.A. Gray, Preparation of mixed-phase titanium dioxide nanocomposites via solvothermal processing, Chemistry of Materials 19 (2007) 1143–1146.
[33] G. Li, S. Ciston, L. Chen, N.M. Dimitrijevic, T. Rajh, K.A. Gray, Synthesizing mixed-phase TiO2 nanocomposites using a hydrothermal method for photooxidation and photoreduction applications, Journal of Catalysis 253 (2008) 105–110.
[34] Y. Ku, C.M. Ma, Y.S. Shen, Decomposition of gaseous trichloroethylene in a photoreactor with TiO_2-coated nonwoven fiber textile, Applied Catalysis B-Environmental 34 (2001) 181–190.
[35] K.N. Timmis, *Pseudomonas putida*: a cosmopolitan opportunist par excellence, Environmental Microbiology 4 (2002) 779–781.
[36] T. Tolker-Nielsen, U.C. Brinch, P.C. Ragas, J.B. Andersen, C.S. Jacobsen, S. Molin, Development and dynamics of *Pseudomonas* sp biofilms, Journal of Bacteriology 182 (2000) 6482–6489.
[37] D.J. Reasoner, E.E. Geldreich, A new medium for the enumeration and subculture of bacteria from potable water, Applied and Environmental Microbiology 49 (1985) 1–7.
[38] D. Scavia, G.A. Laird, G.L. Fahnenstiel, Production of planktonic bacteria near Lake-Michigan, Limnology and Oceanography 31 (1986) 612–626.
[39] D.O. Hessen, E.T. Gjessing, J. Knulst, E. Fjeld, TOC fluctuations in a humic lake as related to catchment acidification, season and climate, Biogeochemistry 36 (1997) 139–151.
[40] D.C. Montgomery, G.C. Runger, Applied Statistics and Probability for Engineers, Wiley, Hoboken, NJ, 2007.
[41] P.Y. Litzler, L. Benard, N. Barbier-Frebourg, S. Vilain, T. Jouenne, E. Beucher, C. Bunel, J.F. Lemeland, J.P. Bessou, Biofilm formation on pyrolytic carbon heart valves: influence of surface free energy, roughness, and bacterial species, Journal of Thoracic and Cardiovascular Surgery 134 (2007) 1025–1032.
[42] S.B.S. Ghayeni, P.J. Beatson, R.P. Schneider, A.G. Fane, Adhesion of waste water bacteria to reverse osmosis membranes, Journal of Membrane Science 138 (1998) 29–42.
[43] L.C. Simoes, M. Simoes, R. Oliveira, M.J. Vieira, Potential of the adhesion of bacteria isolated from drinking water to materials, Journal of Basic Microbiology 47 (2007) 174–183.
[44] Z. Fang, Y.C. Qiu, H. Wang, E. Kuffel, Improving hydrophobicity of glass surface using dielectric barrier discharge treatment in atmospheric air, Plasma Science & Technology 9 (2007) 582–586.
[45] N. Sakai, A. Fujishima, T. Watanabe, K. Hashimoto, Quantitative evaluation of the photoinduced hydrophilic conversion properties of TiO_2 thin film surfaces by the reciprocal of contact angle, Journal of Physical Chemistry B 107 (2003) 1028–1035.
[46] J.R. Garbow, J. Asrar, C.J. Hardiman, Polymer-coated alumina particles—correlation of structure and chromatographic performance, Chemistry of Materials 5 (1993) 869–875.
[47] K.T. Valsaraj, P.M. Jain, R.R. Kommalapati, J.S. Smith, Reusable adsorbents for dilute solution separation. 1: Adsorption of phenanthrene on surfactant-modified alumina, Separation and Purification Technology 13 (1998) 137–145.
[48] M.M. Yee, T. Miyajima, N. Takisawa, Evaluation of amphiphilic properties of fulvic acid and humic acid by alkylpyridinium binding study, Colloids and Surfaces A-Physicochemical and Engineering Aspects 272 (2006) 182–188.
[49] C. Jucker, M.M. Clark, Adsorption of aquatic humic substances on hydrophobic ultrafiltration membranes, Journal of Membrane Science 97 (1994) 37–52.